SINERGI Vol. 26, No. 3, October 2022: 311-318
http://publikasi.mercubuana.ac.id/index.php/sinergi
http://doi.org/10.22441/sinergi.2022.3.006

The real contact width evaluation of a three-layer metal gasket

I Made Gatot Karohika[1*], Shigeyuki Haruyama[2]
[1]Department of Mechanical Engineering, Faculty of Engineering, Universitas Udayana, Indonesia
[2]Graduate School of Innovation and Technology Management, Yamaguchi University, Japan

Abstract
The performance of a three-layer metal gasket is affected by the contact width between the gasket surface and the rough flanges. In the simulation, proper flange roughness modeling will make it easier to predict the gasket performance later. The surface roughness modeling in the simulation will be compared with experimental measurements to determine how much contact occurs due to the rough flange surface. Experimental measurement of real contact width using a digital microscope and simulation using finite element software. The measurements between the simulation results of the real surface roughness model and the experimental results show that they are close to the same. So it can be said that our simulation model is close to the actual conditions.

Keywords:
Contact width;
Flange;
Gasket;
Simulation;
Surface roughness;

Article History:
Received: December 25, 2021
Revised: January 26, 2022
Accepted: February 13, 2022
Published: October 4, 2022

Corresponding Author:
I Made Gatot Karohika, Department of Mechanical Engineering, Universitas Udayana, Indonesia
Email: gatot.karohika@unud.ac.id

INTRODUCTION

A gasket is a component that is placed between the flange connections in the piping system, which aims to prevent leakage, which is affected by imperfections on the flange surface. One of the gaskets that are widely used in metal gaskets. Previous studies have shown that the performance of metal gaskets is influenced by width when contact, large stress when contact [1], and load per length unit [2]. So the researchers tried to optimize these parameters to improve the gasket's sealing performance in minimizing leakage.

Another study also stated that the performance of gaskets was influenced by the surface roughness of the flange and gasket. It stated that with the increase in surface roughness, the contact width value decreased, thereby reducing the performance of the gasket [3].

Due to the surface roughness effect, when the flange is in contact with the gasket due to the effect of the clamping/tightening force, the rough surface of the flange will cause the gasket to be plastically deformed, which shows the width of contact. This is the effective width of the gasket in contact with the flange, and the real contact width prevents leakage. Therefore, several researchers conducted a study of this real contact width to find out the minimum contact width needed to avoid leakage, which is influenced by the surface roughness of the flange with several methods of measuring contact width [4, 5, 6] and contact stress measurement [7]. However, most real-contact measurements are carried out experimentally, which is costly and time-consuming.

With the development of computer technology and software today, it is possible for researchers to model the real condition of the gasket contact and provide analysis more quickly and more economically [8, 9, 10, 11, 12, 13, 14, 15, 16]. But, of course, to be surer that calculations or experiments [17, 18, 19, 20, 21, 22]. The model can represent the actual case conditions. Analytical, this study must validate the results. The researcher wants to look into how the flange's surface roughness affects the actual width of contact of the three-layer gasket, by modelling it using FEM software. The simulation

modelling results are also validated with experimental results in the form of photos digital microscopes. With this validation process, it is hoped that in the future, using a simulation model, the author can predict the actual width of contact for various degrees of surface roughness.

METHOD

Material

The gasket was constructed with SUS304 as the base material, three layers of oxygen-free copper (C1020) as the surface layer, and no bonding. Die dimensions are based on SUS304's ideal design for a single material, which has a 400 MPa and 0 MPa mode. Figure 1 depicts the material gasket before to the forming process and the gasket following the forming process.

Methods

The surface roughness has an impact on sealing effectiveness as well. Figure 2 depicts the measurement configuration for the flange surface roughness. The surface roughness was measured using a Handy Surf E-35B. In order to prevent experimental error caused by the surface roughness, the apparatus was first calibrated. Then, in accordance with the measurement conditions, the measuring range, evaluation, limit value, and recording magnification are automatically determined to get the optimum value. The measurement circumstances, parameter values, and profile data curve will be delivered immediately to the personal computer.

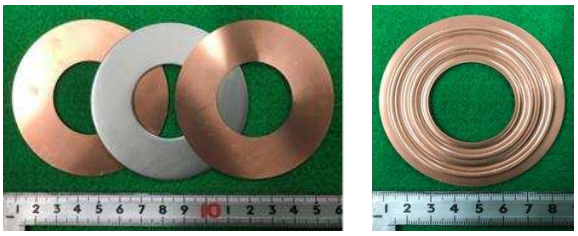

(a) (b)

Figure 1. Material metal gasket (a) before forming (b) after forming

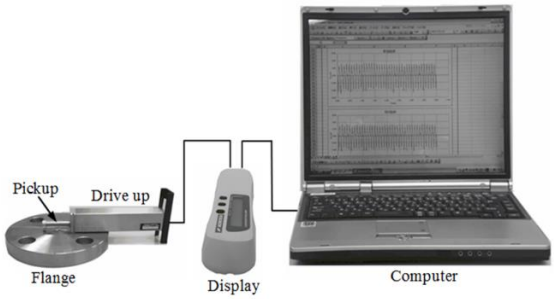

Figure 2. The setup to measurement Surface roughness [5]

Microsoft Excel was used to modify the data. The output findings acquired, including the roughness curve, are the average surface roughness Ra, the maximum surface roughness Rz, and other characteristics. Figure 3 displays an illustration of the surface roughness measuring findings. The average surface roughness (Ra) of the flanges employed in this investigation is 2.5 mm and 3.5 mm. Using SolidWorks software, this data was utilized to depict the actual flange surface roughness.

To explain the contact mechanism between metal gaskets of size 25A and rough flanges, a simulation analysis was done. This method allows for determining the link between the surface roughness, contact stress, and contact breadth parameters. Gaskets are created in research using press moulds. There are beads arranged along the edge. The beads on both of the gasket's faces become elastic when the flanges tighten the gasket. On both sides of the flange, the rough surface is presumptive. The bottom and upper sides of the gasket surface are in contact with the flange, which forces the gasket axially. The flange was made of SS400, the core was made of SUS304, and the surface was made of C1020. Specific material characteristics are listed in Table 1.

In this study, the surface roughness was modeled using CAD software based on the measurement results of the handy Surf E-35B. The flange surface roughness is modeled based on both Ra, and RSM data. The height of the asperities is described based on the average roughness, and the RSM data depict the surface roughness wavelength.

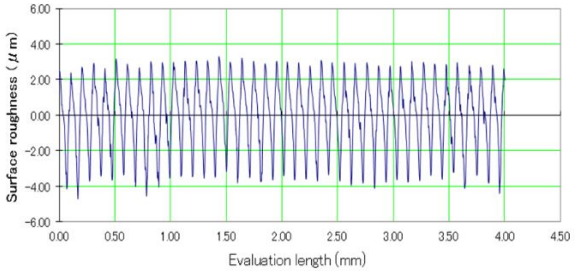

Figure 3. The curve of roughness

. Table 1. Material properties

Materials	Nominal Stress (σ) (Mpa)	Tangent Modulus (Mpa)	Elasticity Modulus (E) (Gpa)	Poisson ratio (v)
SUS304	398.83	1900.53	210	0.3
SS400	240	1000	206	0.3
C1020	195	1360	136	0.31

With the aid of FEM software MSC. Marc, the elastoplastic behavior of the gasket is estimated. The condition of loading is shown in Figure 4. In our study, compression displacement in the axial direction on the gasket between the upper and lower dies and flange with a continuous rising step of displacement is implemented using two-dimensional axisymmetric solid elements of isoparametric quadrilateral type 10.

Figure 5 illustrates the J2-deformation theory of Mises' yield criteria for bilinear stress-strain behavior, which is used in our work to characterize the material. The material is assumed to follow isotropic linear strain hardening. The Newton-Raphson approach is employed to solve the equilibrium equations made up of finite strain plasticity with the multiplicative decomposition of the deformation gradient during our nonlinear analysis using the iterative process.

The contact stress value in the horizontal position can be used to simulate the contact width. No contact is defined as a contact stress value of 0 MPa, elastic contact is defined as a contact stress value between 0-195 MPa, and plastic contact is defined as a contact stress value over 195 MPa. According to Figure 6, the actual contact width is calculated by multiplying the number of vertices having plastic contact stress by the element's diameter.

The contact stress and width were obtained from the simulation results in four stages. The first stage uses SolidWorks software to describe 2-D models of flanges and gaskets. Image files are saved in the form of IGES files. The second stage is the meshing process by utilizing the HyperMesh software. Gasket and flanges are modeled on a rectangular mesh, stored as NAS files.

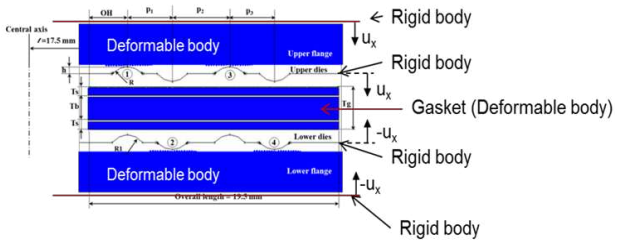

Figure 4. Analysis model

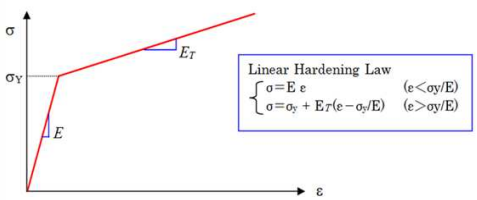

Figure 5. Linear strain hardening model

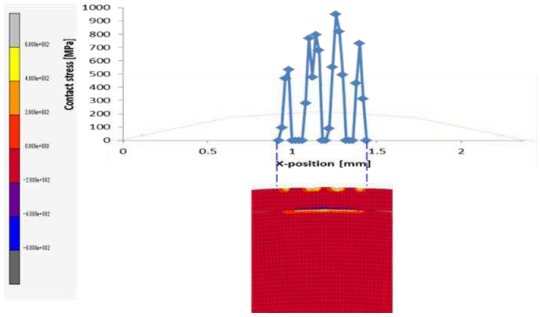

Figure 6. Contact width

Then the data is exported into MSC-marc software for pre-processing and running the model. This is the third stage. In the fourth stage, the output file from the FEA software is converted to a TXT file which Microsoft Excel then processes to get results containing the contact status, contact width, contact stress and force at any time at each position.

Three-layer sheet metal is seen in Figure 7, with Ts denoting the thickness of the surface layer, Tb denoting the thickness of the base metal, and Tg denoting the overall thickness of the gasket. The settings for gasket material, flange, and curve are shown in Figure 8. Figure 8 also depicts the creation of gaskets using dies that mimic a press mould. The contact between the surface layer (C1020) and the base metal (SUS304) is not fixed.

The deformable bodies were assumed on the gasket and the flange. Figure 9 represents the gasket tightening process by the flange.

In this simulation, the thickness ratio [Ts/Tg] fluctuates for the 0MPa mode at 0.1/1.2, 0.2/1.2, and 0.4/1.2. For the 400MPa mode, 0.1/1.5, 0.2/1.5, 0.4/1.5, and 0.5/1.5.

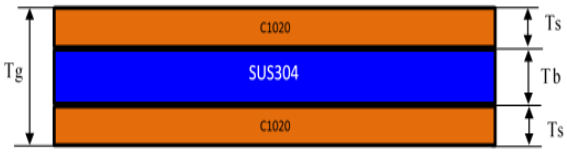

Figure 7. Three-layer sheet metal

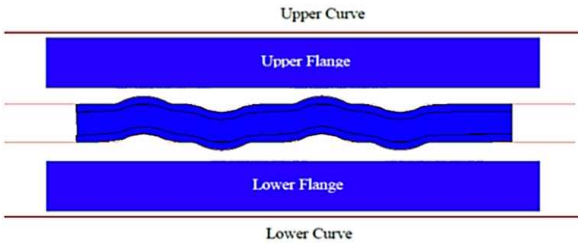

Figure 8. Forming simulation

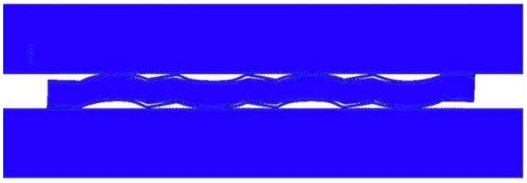

Figure 9. Tightening simulation

RESULTS AND DISCUSSION

Surface gaskets were examined to determine the actual contact width that really happened following the leak test using the helium leak test. A gasket and flange are shown in contact in Figure 10 and after contact. On the convex side of the gasket, a groove is produced, as shown in Figure 10(b). This occurs as a result of the flange surface's roughness during the tightening procedure.

The digital microscope from the VH-Z250 series is set up in Figure 11 to measure contact width. 150X magnification is employed. The overall width of the groove as illustrated in determines the actual breadth of contact between the gasket and the flange (1).

$$CW = \sum_{i=1}^{n} h_i \qquad (1)$$

Figure 12 shows the contact width of the simulation results for the 0MPa mode gasket for a flange surface roughness of 2.5µm and 3.5µm at an axial force of 120kN. Meanwhile, Figure 13 shows the contact width of the simulation results for the 400MPa mode gasket for the flange surface roughness of 2.5µm and 3.5µm at an axial force of 120kN.

Due to the fact that both inner corrugated sections 2 and 3 of the surface layer gasket impact the sealing effectiveness, we assessed them based on the results of the previous study.

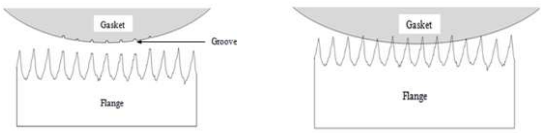

(a) (b)

Figure 10. Gasket contact to flange (a) contact condition and (b) while in touch [5]

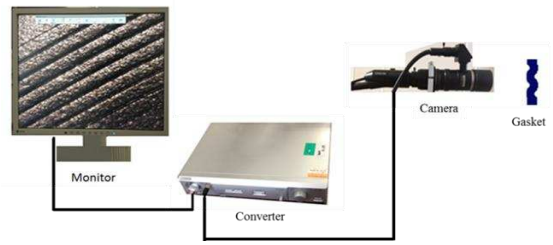

Figure 11. Digital microscope VH-Z250 [5]

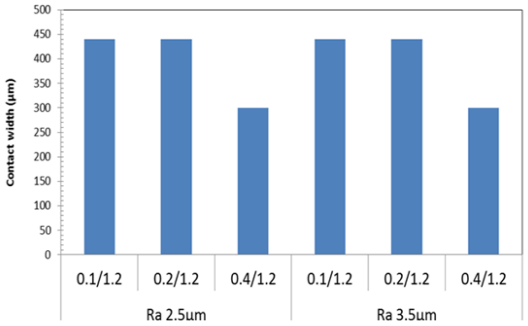

Figure 12. Contact width for gasket 0MPa mode at axial force 120kN [simulation result].

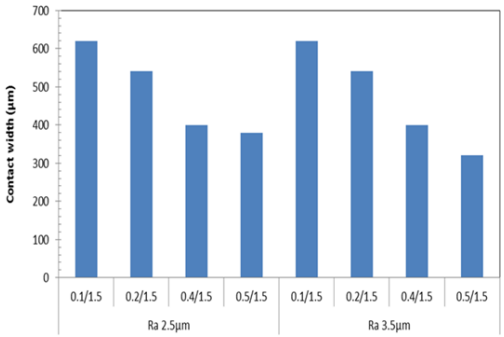

Figure 13. Contact width for gasket 400MPa mode and at axial force 120kN [simulation result].

These corrugated parts have longer contact widths and higher contact stress compared with corrugated portions 1 and 4 [5].

Figure 14 shows a photo showing a groove formed (dark part) on one part representing the surface of the 0MPa mode gasket after contact with the flange, which has a roughness of Ra 2.5µm, and Figure 15 for Ra 3.5µm. While the gasket mode 400MPa is shown in Figure 16 and Figure 17. Based on the photo, with the existing software facilities on the Digital microscope VH-Z250, the width of the groove formed can be measured. The surface layer gasket's actual contact width may then be calculated using (1).

Following the picture measurements, the actual contact width is displayed as a bar chart, as seen in Figure 18 for a 0MPa gasket. For the gasket three-layer no bond concept, a higher thickness ratio results in a smaller contact width. The largest true contact width, for instance, is demonstrated by a gasket with a thickness ratio of 0.1/1.2. Additionally, the contact breadth varies somewhat between the two surface roughnesses. It means that for three-layer gaskets, the impact of surface roughness is negligible.

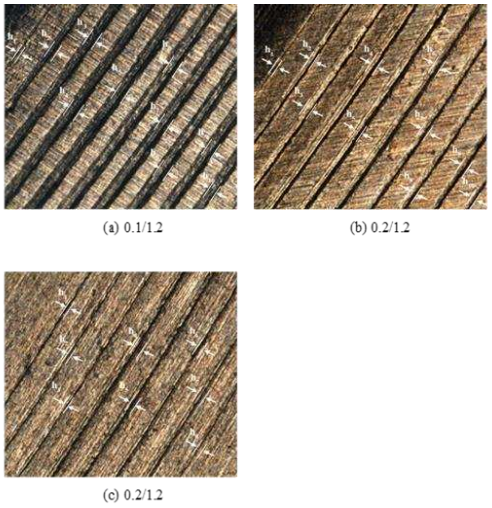

Figure 14. After contact, the gasket's surface roughness is 0-MPa for Ra 2.5 m.

Figure 15. After contact, the gasket's surface roughness is 0-MPa for Ra 3.5μm

Figure 16. After contact, the gasket's surface roughness is 400-MPa for Ra 2.5 m.

Figure 17. Surface roughness of the gasket at 400 MPa following contact for Ra 3.5 m

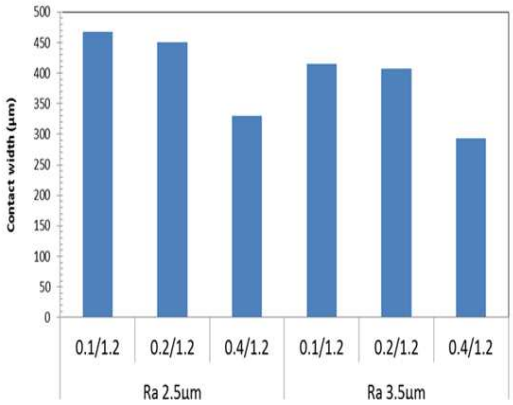

Figure 18. Results of the actual contact width experiment for all levels of the flange's real surface roughness model at all thickness ratios [0MPa-mode]

As illustrated in Figure 19, the true contact width for the 400MPa gasket, which was determined from the picture measurements, is displayed as a bar chart. For the gasket three-layer no bond concept, a higher thickness ratio results in a smaller contact width. The largest true contact width, for instance, is demonstrated by a gasket with a thickness ratio of 0.1/1.5. The contact breadth between the two surface roughnesses is slightly varied. It means that for three-layer gaskets, the impact of surface roughness is negligible.

Figure 20 and Figure 21 compare the contact width between simulation and experiment for three-layer gaskets operating in 0 MPa and 400 MPa modes. These figures indicate a trend in the contact width that is comparable. In comparison to the gasket 0MPa mode, the true contact width for the gasket 400MPa mode was greater. The effect of surface roughness is minimal.

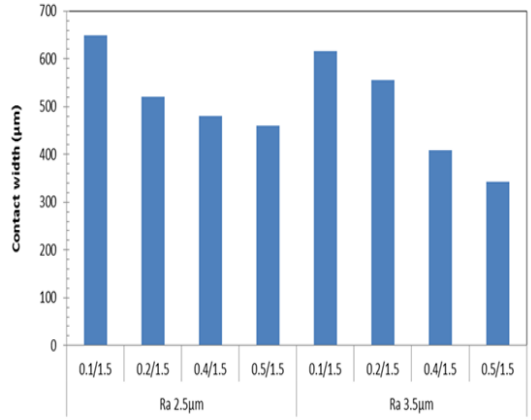

Figure 19. Results of the actual contact width experiment for all levels of the flange's real surface roughness model and all thickness ratios (400 MPa mode)

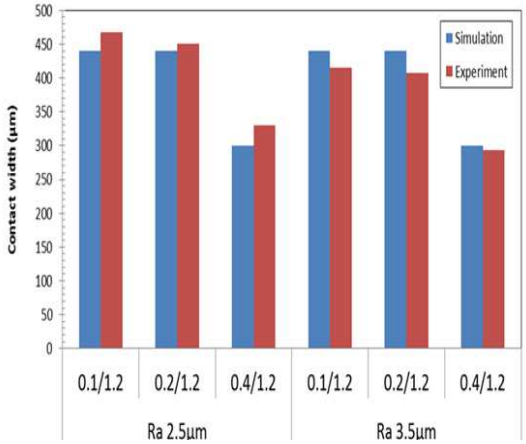

Figure 20. Contact width variations between simulation and experiment in the gasket 0MPa mode

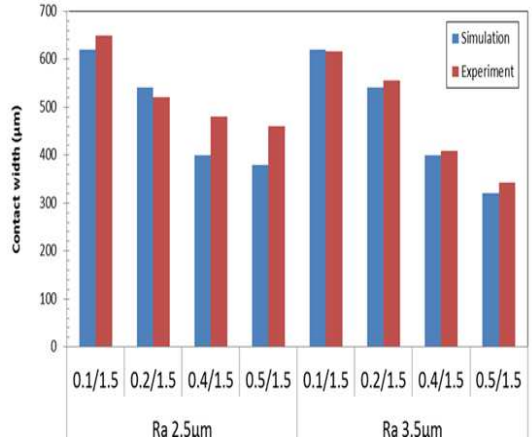

Figure 21. Contact width variations between simulation and experiment in the 400 MPa mode

Table 2 and Table 3 show the simulation and experimental results for the 0-MPa gasket mode, for the surface roughness Ra 2.5µm and Ra 3.5µm. According to Table 4, the overall difference in real contact width measurement between the experiment's data and the simulation's data for the gasket's 0-MPa mode is 5.62%.

Table 5 and Table 6 show the simulation and experimental results for the 400-MPa gasket mode, for the surface roughness Ra 2.5µm and Ra 3.5µm.

Table 2. Gasket 0MPa mode, Ra 2.5 modeling results and experiment differences

	Ra 2.5		
	0.1/1.2	0.2/1.2	0.4/1.2
Simulation result (µm)	440	440	300
Experimental result (µm)	467.8375	450.19125	330.5225
Differences (%)	5.95	2.26	9.23
Average %		5.82	

Table 3. Gasket 0MPa mode, Ra 3.5 modeling results and experiment differences

	Ra 3.5		
	0.1/1.2	0.2/1.2	0.4/1.2
Simulation result (µm)	440	440	300
Experimental result (µm)	414.8475	407.89875	293.1
Differences (%)	6.06	7.87	2.35
Average %		5.43	

Table 4. The total average discrepancies between the experiment's gasket 0MPa mode and simulation results

	Ra 2.5	**Ra 3.5**
Average %	5.82	5.43
Total Average %	5.62	

Table 5. Contact width differences between simulation results and experiment results for the 400 MPa mode, Ra 2.5

	Ra 2.5			
	0.1/1.5	0.2/1.5	0.4/1.5	0.5/1.5
Simulation result (µm)	620	540	400	380
Experimental result (µm)	649.13	521.0154	479.54	460.53
Differences (%)	4.49	3.64	16.59	17.49
Average %		10.55		

Table 6. Contact width differences between simulation results and experiment results for the 400 MPa mode, Ra 3.5

	Ra 3.5			
	0.1/1.5	0.2/1.5	0.4/1.5	0.5/1.5
Simulation result (μm)	620	540	400	320
Experimental result (μm)	615.5	555.56	409.36	343.57
Differences (%)	0.73	2.80	2.29	6.86
Average %	3.17			

Table 7. The total average discrepancies between the experiment's gasket 400MPa mode and simulation results

	Ra 2.5	Ra 3.5
Average %	10.55	3.17
Total average %	6.86	

However, Table 7 listed the comparison of the experiment and simulation results for the gasket 400-MPa mode, reveals a total variance in true contact width measurement of 6.86%. Using these data, we may utilize simulation modeling to simulate the flanges' surface roughness and estimate the actual contact width of the resultant contact, reducing the expense and duration of experimental testing.

CONCLUSION

As previously stated, the goal of this study is to model the 3-layer gasket using FEM software and experimental data in the form of photographs in order to ascertain its actual contact width, which is influenced by the flange's surface roughness. It is derived from a simulation that demonstrates that the contact width of a three-layer gasket in 400MPa mode is greater than that in 0MPa mode. We can say that our simulation model comes close to the real model since the overall measurement disparities between the simulation result using the real surface roughness model and the experimental result are negligible. Therefore, in the future, the real surface roughness can model using simulation to get the real contact width result.

ACKNOWLEDGMENT

Universitas Udayana supported this research through LPPM and Strength of Material Laboratory, Yamaguchi University.

REFERENCES

[1] D. Nurhadiyanto, S. Haruyama, K. Kaminishi, I. M. Gatot Karohika, and D. Mujiyono, "Contact Stress and Contact Width Analysis of Corrugated Metal Gasket," *Applied Mechanics and Materials*, vol. 799–800, pp. 765–769, 2015, doi: 10.4028/www.scientific.net/AMM.799-800.765

[2] I. M. G. Karohika *et al.*, "An Approach to Optimize the Corrugated Metal Gasket Design Using Taguchi Method," *International Journal on Advanced Science, Engineering and Information Technology,* vol. 10, no. 6, pp. 2435–2440, 2020, doi: 10.18517/ijaseit.10.6.12992

[3] S. Haruyama, D. Nurhadiyanto, M. A. Choiron, and K. Kaminishi, "Influence of surface roughness on leakage of new metal gasket," *International Journal of Pressure Vessels and Piping*, vol. 111-112, pp. 146-154, 2013, doi: 10.1016/j.ijpvp.2013.06.004

[4] Y. Xu, Y. Chen, A. Zhang, R. L. Jackson, and B. C. Prorok, "A New Method for the Measurement of Real Area of Contact by the Adhesive Transfer of Thin Au film," *Tribology Letters*, vol. 66, no. 1, 2018, doi: 10.1007/s11249-018-0982-5

[5] S. Maegawa, F. Itoigawa, and T. Nakamura, "Optical measurements of real contact area and tangential contact stiffness in rough contact interface between an adhesive soft elastomer and a glass plate," *Journal of Advanced Mechanical Design, Systems, and Manufacturing*, vol. 9, no. 5, pp. 1-14, 2015, doi: 10.1299/jamdsm.2015jamdsm0069

[6] L. T. Li, X. M. Liang, Y. Z. Xing, D. Yan, and G. F. Wang, "Measurement of real contact area for rough metal surfaces and the distinction of contribution from elasticity and plasticity," *Journal of Tribology*, vol. 143, no. 7, pp. 1–23, 2021, doi: 10.1115/1.4048728

[7] M. Zhang, S. Suo, Y. Jiang, G. Meng, "Experimental Measurement Method for Contact Stress of Elastic Metal Sealing Ring Based on Pressure Sensitive Paper," *Metals*, vol. 8, no. 11, pp. 942, 2018, doi: 10.3390/met8110942

[8] I. M. G. Karohika and I. N. G. Antara, "Proses Pembentukan Gasket berlapis dengan Metode Elemen Hingga," *Jurnal Energi Dan Manufaktur*, vol. 11, no. 2, pp. 62-66, 2018, doi: 10.24843/jem.2018.v11.i02.p06

[9] I. M. G. Karohika, S. Haruyama, I. N. G. Antara, I. N. Budiarsa, and I. M. D. B. Penindra, "Sealing Performance Layered Metal Gasket Based on the Simulation Method," *Teknik*, vol. 41, no. 1, pp. 14–19, 2020, doi: 10.14710/teknik.v41i1.26125

[10] I. N. Budiarsa, I. N. G. Antara, I. M. G. Karohika, I. W. Widhiada, and N. L.

Watiniasih, "Identification Plastic Properties of Spot Welded Joints Using the Instrumented Indentation Technique," *IOP Conference Series: Materials Science and Engineering*, vol. 811, no. 1, pp. 0–5, 2020, doi: 10.1088/1757-899X/811/1/012020

[11] W. Widhiada, I. N. G. Antara, I. N. Budiarsa, and I. M. G. Karohika, "The Robust PID Control System of Temperature Stability and Humidity on Infant Incubator Based on Arduino at Mega 2560," in *IOP Conference Series: Earth and Environmental Science*, 2019, doi: 10.1088/1755-1315/248/1/012046

[12] I. M. G. Karohika and I. N. G. Antara, "Gasket Process Parameter in Metal Forming," in *IOP Conference Series: Earth and Environmental Science*, 2019, doi: 10.1088/1755-1315/248/1/012044

[13] I. N. Budiarsa, I. M. Astika, I. N. G. Antara, and I. M. G. Karohika, "Optimization on strength spot welding joint trough finite element modelling indentation approach," *IOP Conference Series: Earth and Environmental Science*, vol. 539, no. 1, 2019, doi:10.1088/1757-899X/539/1/012042

[14] I. M. G. Karohika, I. N. G. Antara, and I. M. D. Budiana, "Influence of dies type for gasket forming shape," in *IOP Conference Series: Materials Science and Engineering*, 2019, doi: 10.1088/1757-899X/539/1/012019

[15] I. M. G. Karohika and I. N. G. Antara, "The metal gasket sealing performance of bolted flanged with fem analysis," in *IOP Conference Series: Materials Science and Engineering*, 2019, doi: 10.1088/1757-899X/539/1/012018

[16] I. N. Budiarsa, I. N. G. Antara, and I. M. G. Karohika, "Indentation Size Effect of the Vickers Indentation to Improve the Accuracy of Inverse Materials Properties Modelling Based on Hardness Value," in *IOP Conference Series: Earth and Environmental Science*, 2019, doi: 10.1088/1755-1315/248/1/012009

[17] S. Haruyama, M. A. Choiron, and D. Nurhadiyanto, "Optimum Design of Laminated Corrugated Metal Gasket Using Computer Simulation", *International Journal of Integrated Engineering*, vol. 11, no. 5, pp. 29–34, 2019

[18] D. Nurhadiyanto, Mujiyono, Sutopo, and F. Amri Ristadi, "Simulation Analysis of 25A-Size Corrugated Metal Gasket Coated Copper to Increase Its Performance," *IOP Conference Series: Earth and Environmental Science*, vol. 307, p. 012005, 2018, doi: 10.1088/1757-899X/307/1/012005

[19] D. Nurhadiyanto, S. Haruyama, Mujiyono, and Sutopo, "An analysis of changes in flange surface roughness after being used to tighten a corrugated metal gasket," *IOP Conference Series: Earth and Environmental Science*, vol. 535, no. 1, 2019, doi: 10.1088/1757-899X/535/1/012015

[20] A. Fitriadhy, N. A. Adam, and C. J. Quah, "Computational Prediction of a Propeller Performance In Open Water Condition," *SINERGI*, vol. 24, no. 2, pp. 163-170, 2020, doi: 10.22441/sinergi.2020.2.010.

[21] B. Mulyanto and D. S. Khaerudini, "Simulation and Experimental Investigation of Wrinkle Defect in Deep Drawing Process of Carbon Steel Spcc Shaped Cylinder Flange Cup," *SINERGI*, vol. 24, no. 3, pp. 197-206, 2020, doi: 10.22441/sinergi.2020.3.004.

[22] I. M. G. Karohika and S. Haruyama, "Analysis of three-layer gasket performance affected by flange surface", *EUREKA: Physics and Engineering*, no. 4, pp. 57-66, 2022, doi: 10.21303/2461-4262.2022.002290